

CORRESPONDENCE

Open Access



Pharmacological activity of OST-01, a natural product from *Baccharis coridifolia*, on breast cancer cells

HyunJun Kang^{1†}, Dinh Hoa Hoang^{1†}, Melissa Valerio¹, Khyatiben Pathak², William Graff³, Alexis LeVee⁴, Jun Wu⁵, Mark A. LaBarge⁶, David Frankhouser⁷, Russell C. Rockne⁷, Patrick Pirrotte², Bin Zhang¹, Joanne Mortimer⁴, Le Xuan Truong Nguyen^{1,2*} and Guido Marcucci^{1*}

Abstract

Natural products have long been a viable source of therapeutic agents, providing unique structures and mechanisms that may be beneficial for cancer treatment. Herein we first report on the anticancer activity OST-01, a natural product from *Baccharis Coridifolia*, on breast cancer cells, including triple-negative breast cancer (TNBC). OST-01 significantly inhibited cell proliferation and oncogenic activities of TNBC cells in vitro. OST-01 also markedly inhibited TNBC tumor growth in vivo, with > 50% reduction in tumor size compared to vehicle control treatment in different in vivo models, i.e., cell line-derived (CDX), patient-derived (PDX), and mammary fat pad xenografts. Mechanistically, OST-01 induces ferroptosis by downregulating LRP8-regulated selenoproteins, i.e., GPX4. A shift from a basal-mesenchymal to a luminal-epithelial state of breast cancer stem cells (BCSCs) as supported by the downregulation of stemness (e.g., CD44) and mesenchymal (e.g., FN1 and vimentin) markers, along with the upregulation of differentiation markers (e.g., CD24) and luminal-epithelial markers (e.g., CK19), was also observed.

Keywords TNBC, BCSC, Natural product, OST-01, Ferroptosis

[†]HyunJun Kang and Dinh Hoa Hoang authors contribute equally to this study.

*Correspondence:
Le Xuan Truong Nguyen
lenguyen@coh.org
Guido Marcucci
gmarcucci@coh.org

¹Department of Hematologic Malignancies Translational Science, Beckman Research Institute and City of Hope National Medical Center, Duarte, CA, USA

²Early Detection and Prevention Division, Translational Genomics Research Institute, Phoenix, AZ, USA

³Ostentus Therapeutics, Inc, Newport Coast, CA, USA

⁴Division of Medical Oncology and Experimental Therapeutics, Beckman Research Institute and City of Hope National Medical Center, Duarte, CA, USA

⁵City of Hope Comprehensive Cancer Center, Duarte, CA, USA

⁶Department of Population Sciences, Beckman Research Institute and City of Hope National Medical Center, Duarte, CA, USA

⁷Department of Computational and Quantitative Medicine, Division of Mathematical Oncology, Beckman Research Institute and City of Hope National Medical Center, Duarte, CA 91010, USA



To the Editor,

Natural products (NPs) have been essential in cancer drug discovery, with noteworthy examples of plant-derived chemotherapeutics currently part of stand-of-care regimens [1]. *Baccharis (B) coridifolia*, a South American plant of the Asteraceae family, is used in botanical medicine without reported toxicity in humans [2]. We previously showed that OST-01, a NP derived from *B. coridifolia*, has in vivo efficacy in acute myeloid leukemia (AML) by disrupting c-Myc-dependent ribogenesis of leukemic stem cells [3]. Herein we report that OST-01 is also cytotoxic to a variety of solid tumors, including lung, colon, ovarian, glioblastoma, pancreatic, and breast cancers (Sup. Figure S1A). To this end, we investigated the activity of OST-01 in breast cancer (BC), including triple-negative breast cancer (TNBC), an aggressive subtype enriched with breast cancer stem cells (BCSCs) [4–6].

OST-01 effectively inhibited proliferation of triple-positive BT474 and TNBC (MDA-MB-231, MDA-MB-468, BT549, and 4T1) cells, with IC₅₀ values up to 3.8 $\mu\text{L}/\text{mL}$ (Sup. Figure S1B). At 1 $\mu\text{L}/\text{mL}$, OST-01 also suppressed proliferation and induced apoptosis in patient-derived TNBC cells while sparing normal human mammary epithelial cells (HMECs, Fig. 1A–B). Of note, the proapoptotic activity of OST-01 in triple-positive and TNBC cells appeared stronger than that of other standard-of-care chemotherapeutics (i.e., Taxol and 5-FU), used at concentrations known to demonstrate in vitro activity in inducing apoptosis in cancer cells (Fig. 1C and Sup. Figure S1C). OST-01 also inhibited colony formation, anoikis resistance, wound healing, and invasion (Fig. 1D and Sup. Figure 2 A–D), reduced spheroid formation, and increased TNBC cell death in 3D cultures (Sup. Figure 2E). The in vivo activity of OST-01 was tested in four murine models: a triple-positive BC CDX (BT474), a TNBC CDX (MDA-MB-231), a TNBC PDX, and a luciferase-expressing MDA-MB-231 fat pad xenograft. Mice received either vehicle or OST-01 (1 $\mu\text{L}/\text{g}$, BID) via oral gavage starting 14 days post-injection. After 5 weeks, OST-01 reduced tumor volumes by at least 50% across all models, with p-values of 0.0024 for the BT474 CDX, 0.0019 for the MDA-MB-231 CDX, and 0.0017 for the TNBC PDX (Fig. 1E–G). In the fat pad model, bioluminescence imaging and tumor measurements confirmed approximately 50% reduction in tumor size and weight ($p = 0.0002$, Fig. 1G), validating OST-01's in vivo efficacy.

To investigate OST-01's anticancer mechanism, we performed RNA sequencing on BT474 (triple-positive) and two TNBC cell lines (4T1, MDA-MB-231) treated with ethanol control or OST-01 (1 $\mu\text{L}/\text{mL}$). OST-01 upregulated genes involved into inflammatory response and TNF α /IL6/JAK/STAT3 signaling, while downregulating those related to cell cycle, ROS, mTORC, and Myc

pathways (Sup. Figure 3 A–B). OST-01 notably downregulated BCSC-associated genes, including LRP8, RAD54L, STC-1, SDC-1, and SRSF3 (Fig. 2A–B and Sup. Figure 3 C–E), indicating its targeted action on BCSCs.

Focusing on TNBC cells, we observed that OST-01 downregulated LRP8 (ApoER2), a key regulator of ferroptosis—a process crucial for cancer cell survival, characterized by lipid peroxidation, elevated malondialdehyde (MDA), and decreased GPX4 activity [7, 8]. LRP8 promotes translation of selenoproteins (SELS) like GPX4 by promoting selenium uptake [9–12]. Increased SEL production prevents ferroptosis and supports cancer cell homeostasis [7, 8]. Coessentiality network analysis of the RNA-seq data from OST-01-treated TNBC cells showed the association of LRP8 with SELs, selenocysteine metabolism, and ferroptosis (Sup. Figure 4 A). Gene ontology linked LRP8 downregulation to oxidative stress and glutathione metabolism (Sup. Figure 4B). OST-01 treatment led to increased lipid peroxidation, elevated MDA levels, and decreased GPX4, (Fig. 2C), along with reduced SELs expression (Fig. 2D and Sup. Figure S5A), confirming triggered ferroptosis. In vivo, BC cells from OST-01-treated xenografts showed lower SDC1, LRP8, and GPX4 levels than controls (Sup. Figure S5B). Additionally, LRP8 overexpression (OE) in MDA-MB-231 TNBC cells conferred resistance to OST-01, increasing proliferation and reducing ferroptosis (Fig. 2E–F) and resulting in larger tumors in xenografts (Fig. 2G), supporting LRP8's role in OST-01-induced ferroptosis. Of note, GSEA indicates that OST-01 treatment promotes a shift in TNBC and triple-positive BC cells from a basal-mesenchymal to a luminal-epithelial state, with reduced CD44 and increased CD24 expression in MDA-MB-231 cells (Fig. 2H–J and Sup. Figure 6). To confirm these findings, we showed that OST-01 reduced mesenchymal markers (FN1, vimentin) and increased CK19, a luminal-epithelial marker (Fig. 2I–J).

In conclusion, we first report on the activity of a novel natural product, OST-01, on TNBC. OST-01 induces ferroptosis by downregulating LRP8 and affecting key pathways related to BCSCs (Fig. 2K), demonstrating potential for overcoming resistance mechanisms in TNBC. The OST-01 unique activity to target BCSC-associated pathways and induce LRP8-dependent ferroptosis along with an expect safe toxicity profile (based on the phytomedicinal use of *B. coridifolia* in South America) underscores its clinical potential. Further investigations into mechanisms of action and synergistic combinations with other therapeutics are warranted to address treatment-resistant challenges encountered by current treatment regimens.

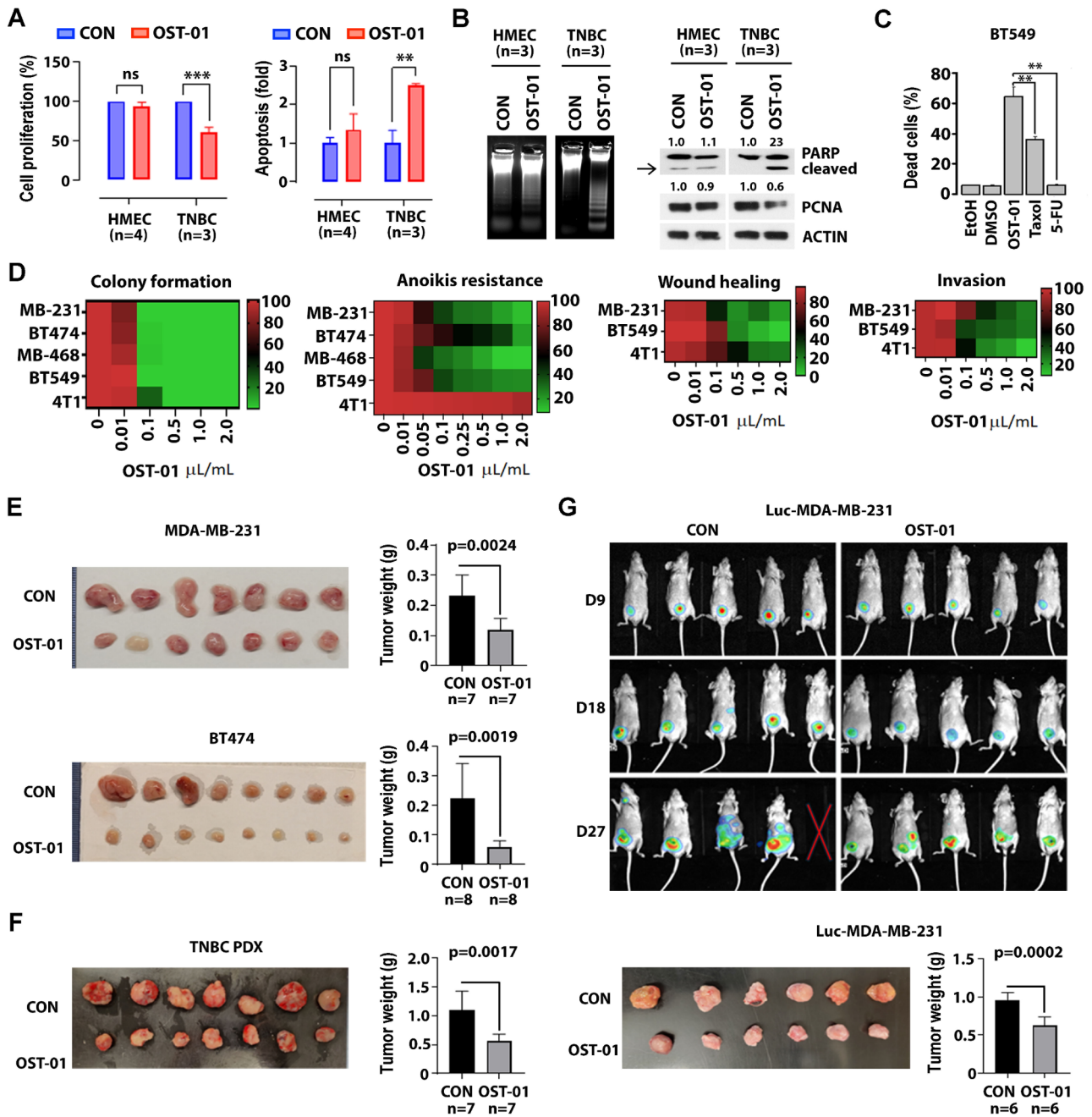


Fig. 1 Effects of OST-01 on oncogenic activities in TNBC cells in vitro and tumor growth in vivo. **A-B** Effects of OST-01 on proliferation and apoptosis in primary HMEC and TNBC cells. Primary HMEC ($n=4$) and TNBC ($n=3$) cells were treated with 1 μL /mL of ethanol control or OST-01 (1 μL of OST-01 extract contains 250 μg of dry plant extract) for 24 h. **A** Levels of cell proliferation (left) and apoptosis (right). **B** DNA fragmentation (left) and levels of PCNA and PARP cleavage (right). Quantification of protein expressions are shown on top. **C** Comparative effects of OST-01 and other therapeutic drugs on BT549 TNBC cell lines. The cells were treated with 1 μL /mL of OST-01 or 2 μM of Taxol or 5-FU for 24 h. Apoptosis was measured by Annexin V staining. **D** Effects of OST-01 on oncogenic activities in TNBC cells. The indicated triple-positive BC cell line (BT474) and TNBC cell lines [MDA-MB-231 (MB-231), MDA-MB-468 (MB-468), 4T1, and BT549] were treated with increasing doses of OST-01 for 24 h. From left to right: heatmap displaying colony formation, anoikis resistance, wound healing, and invasion levels. **E-G** Effects of OST-01 on TNBC tumor growth in vivo. **E** MDA-MB-231 TNBC cells or BT474 triple-positive BC cells (10^6 cells) were subcutaneously injected into nude mice. After 2 weeks, the transplanted mice were treated with ethanol control or OST-01 (1 $\mu\text{L}/\text{g}$, oral gavage, BID) for 5 weeks. Left, image of isolated tumors. Right, tumor weights (MDA-MB-231: each group, $n=7$; BT474: each group, $n=8$). **F** Primary TNBC-PDX tumors (HCl-023) were subcutaneously transplanted into NSG mice. After 2 weeks, the transplanted mice were treated with ethanol control or OST-01 (1 $\mu\text{L}/\text{g}$, oral gavage, BID) for 5 weeks. Left, image of isolated tumors. Right, tumor weights (each group, $n=7$). **G** Mammary fat pad model using Luc-MDA-MB-231 TNBC cells. 10^6 luciferase (Luc)-expressing MDA-MB-231 cells were injected into the mammary fat pad of NSG mice (each group, $n=10$). After 7 days, the mice were treated with ethanol control or OST-01 (1 $\mu\text{L}/\text{g}$, oral gavage, BID). Top, luminescence images taken on days 9, 18, and 27 after treatment. Bottom, image of isolated tumors (left) and tumor weights (right) (each group, $n=6$)

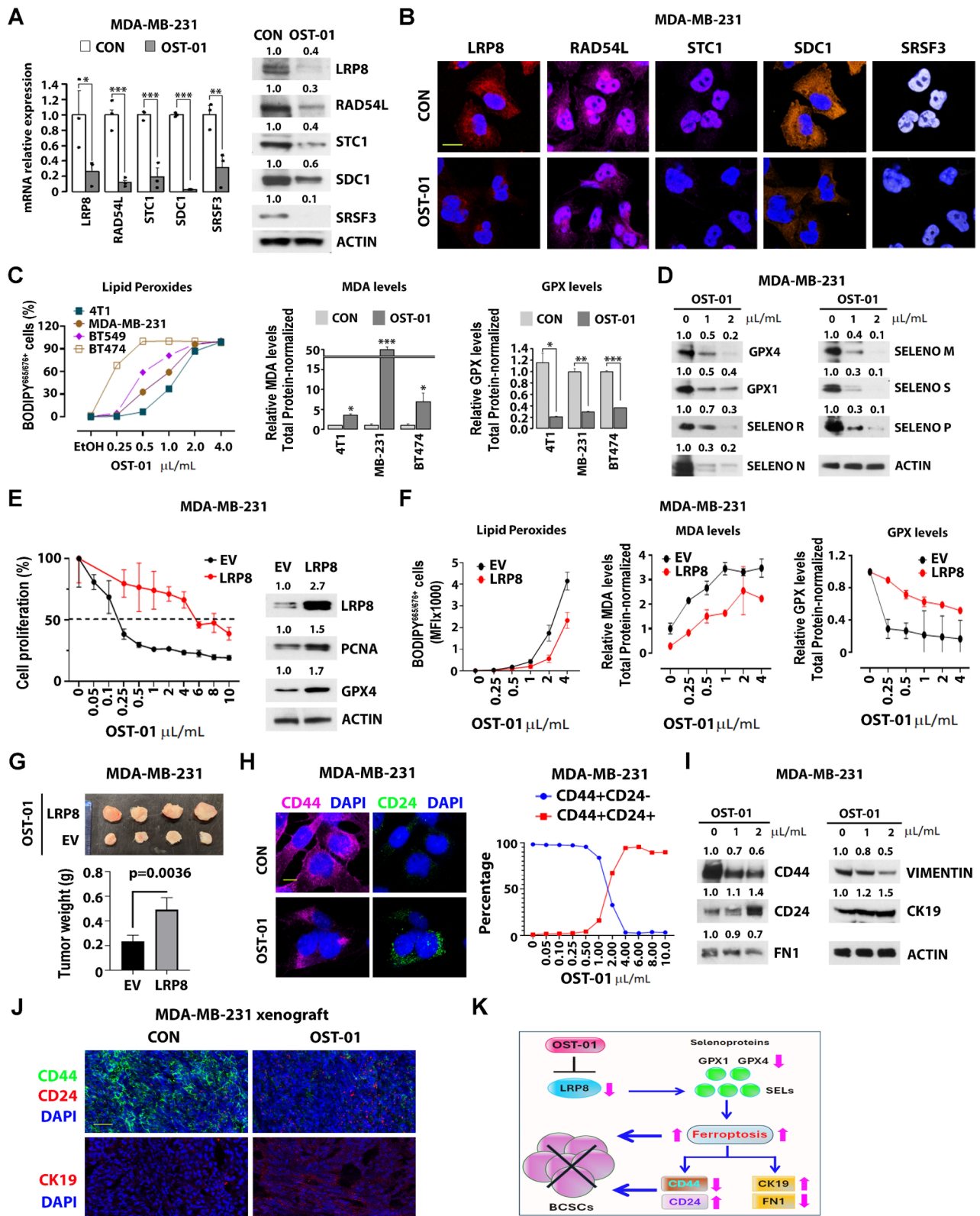


Fig. 2 (See legend on next page.)

(See figure on previous page.)

Fig. 2 Effects of OST-01 on LRP8-regulated ferroptosis in TNBC cells. **A–B** Effects of OST-01 on the expression of key regulators of BCSC. MDA-MB-231 cells were treated with 1 μ L/mL of ethanol control or OST-01 (1 μ L of OST-01 extract contains 250 μ g of dry plant extract) for 24 h. **A** Left, mRNA levels were measured by qPCR. Right, protein levels were measured by immunoblotting. Quantification of protein expressions are shown on top. **B** The treated cells were stained with the indicated antibodies; representative confocal images are shown. Scale bar, 10 μ m. **C** Effects of OST-01 on ferroptosis in TNBC cells. The indicated TNBC cell lines (4T1, MDA-MB-231, and BT549) and the triple-positive BC cell line BT474 were treated with OST-01 in a dose-dependent manner for 24 h. Left: Lipid peroxide levels were measured using a lipid peroxidation assay. Middle: Malondialdehyde (MDA) levels were assessed. Right: Glutathione peroxidase (GPX) levels were measured by a GPX activity assay. **D** Effects of OST-01 on selenoprotein expression in TNBC cells. MDA-MB-231 TNBC cells were treated with OST-01 in a dose-dependent manner for 24 h. Cell lysates were immunoblotted with the indicated selenoprotein antibodies. Quantification of protein expressions are shown on top. **E–G** Effects of LRP8 overexpression on OST-01-induced ferroptosis and TNBC cell growth inhibition. **E** MDA-MB-231 TNBC cells with empty vector control or LRP8 overexpression were treated with OST-01 in a dose-dependent manner for 24 h. Left, cell proliferation was assessed. Right, immunoblotting with the indicated antibodies was performed. Quantification of protein expressions are shown on top. **F** MDA-MB-231 TNBC cells with empty vector control or LRP8 overexpression were treated with OST-01 in a dose-dependent manner for 24 h. Levels of ferroptosis were measured. Left, lipid peroxides levels. Middle, MDA levels. Right, GPX levels. **G** 10^6 MDA-MB-231 TNBC cells with empty vector control or LRP8 overexpression were subcutaneously injected into nude mice. After 2 weeks, the transplanted mice were treated with OST-01 (1 μ L/g, oral gavage, BID) for 5 weeks. Left, image of tumors. Right, tumor weight (each group, $n=4$). **H** Effects of OST-01 on CD44 and CD24 expression. MDA-MB-231 TNBC cells were treated with 1 μ L/mL of ethanol control or OST-01 for 24 h. Left, the treated cells were stained with anti-CD44 (pink) and anti-CD24 (green) antibodies. Images were captured using confocal microscopy. Scale bar, 10 μ m. Right, graph showing the changes in CD44 + CD24- and CD44 + CD24 + populations upon OST-01 treatment. **I–J** Effects of OST-01 on BCSCs in vitro and in vivo. **I** MDA-MB-231 TNBC cells were treated with OST-01 in a dose-dependent manner for 24 h. Cell lysates were immunoblotted with the indicated antibodies. Quantification of protein expressions are shown on top. **J** MDA-MB-231 xenograft tumors isolated from mice treated with ethanol control or OST-01 (as described in Fig. 1E) were subjected to frozen sectioning and stained with the indicated antibodies. Images were captured using confocal microscopy. Scale bar, 1 μ m. **K** Schematic model of the mechanism of action of OST-01 on TNBC cells. OST-01 inhibits LRP8 expression, leading to reduced levels of selenoproteins, including GPX4. The decrease in selenoproteins induces ferroptosis, which in turn suppresses the stemness activities of BCSCs. This effect is achieved through the induction of mesenchymal-to-epithelial transition, resulting in enhanced differentiation of the cells

Abbreviations

AML	Acute Myeloid Leukemia
LSCs	Leukemia stem cells
TNBC	Triple-negative breast cancer
BCSC	Breast cancer stem cells
SEL	Selenoproteins
NP	Natural products
HER	Human epidermal growth factor receptor
ROS	Reactive oxygen species
MOA	Mechanism of action
GSEA	Gene set enrichment analysis
PCNA	Proliferating cell nuclear antigen
HSC	Hematopoietic stem cell
MNC	Mononuclear cell
HMEC	Human mammary epithelial cell
PDX	Patient-derived xenograft
WST-1	Water-soluble tetrazolium salt
FDR	False discovery rate
NES	Normal enrichment score

Supplementary Information

The online version contains supplementary material available at <https://doi.org/10.1186/s13045-025-01668-4>.

Supplementary Material 1
Supplementary Material 2
Supplementary Material 3
Supplementary Material 4
Supplementary Material 5
Supplementary Material 6
Supplementary Material 7
Supplementary Material 8

Acknowledgements

This study was partially supported by the Cherng Family Center for Integrative Oncology Research Pilot Program. We acknowledge the support of the

Animal Resources Center, and the Analytical Cytometry, Bioinformatics, Light Microscopy, Integrative Genomics, and DNA/RNA Cores at City of Hope Comprehensive Cancer Center, funded by the National Cancer Institute of the National Institutes of Health under award number P30CA33572. We are grateful to City of Hope Comprehensive Cancer Center, the patients, and their physicians for providing patient material for this study. We also extend our thanks to Dr. Alana Welm and the Preclinical Research Resource at the University of Utah for supplying primary TNBC samples.

Author contributions

H.K., D.H.H., M.V., K.P., A.L., J.W., D.F., and B.Z., conducted experiments; R.R., P.P., J.M., L.X.T.N., and G.M. reviewed data and the manuscript; W.G. provided OST-01; J.W. provided primary human TNBC samples; M.L. provided HMEC cells; L.X.T.N. and G.M. designed experiments, analyzed data, wrote manuscript and provided administrative support. All authors read and approved the final manuscript.

Funding

This study was partially supported by the Cherng Family Center for Integrative Oncology Research Pilot Program. Additional support was provided by the Animal Resources Center, and the Analytical Cytometry, Bioinformatics, Light Microscopy, Integrative Genomics, and DNA/RNA Cores at City of Hope Comprehensive Cancer Center, funded by the National Cancer Institute of the National Institutes of Health under award number P30CA33572.

Data availability

No datasets were generated or analysed during the current study.

Declarations

Ethics approval and consent to participate

For primary human samples, normal HMEC and TNBC samples were obtained from healthy donors and patients at the City of Hope National Medical Center (COHNMC) under City of Hope Institutional Review Board-approved banking protocols (#07047), or received from the Huntsman Cancer Institute (Utah, USA). All procedures were conducted in accordance with assurances filed with and approved by the Department of Health and Human Services and met the requirements of the Declaration of Helsinki.

For animal studies, all mice were maintained in an Association for Assessment and Accreditation of Laboratory Animal Care (AAALAC) accredited facility, and all experimental procedures adhered to federal and state government guidelines as well as institutional protocols approved by the Institutional Animal Care and Use Committee at City of Hope (IACUC #22043).

Competing interests

W.G., L.X.T.N., and G.M. are shareholders of Ostentus Therapeutic Inc. The remaining authors declare that there is no conflict of interest regarding the publication of this article.

Received: 12 November 2024 / Accepted: 28 January 2025

Published online: 07 February 2025

References

1. Asma ST, Acaroz U, Imre K et al. Natural Products/Bioactive compounds as a source of Anticancer drugs. *Cancers (Basel)*. 2022;14(24).
2. Freitas PR, de Araújo ACJ, dos Santos Barbosa CR, et al. Characterization and antibacterial activity of the essential oil obtained from the leaves of *Baccharis coridifolia* DC against multiresistant strains. *Microb Pathog*. 2020;145:104223.
3. Kang H, Hoang DH, Valerio M, et al. OST-01, a natural product from *Baccharis coridifolia*, targets c-Myc-dependent ribogenesis in acute myeloid leukemia. *Leukemia*. 2024;38(3):657–62.
4. Perou CM, Sørlie T, Eisen MB, et al. Molecular portraits of human breast tumours. *Nature*. 2000;406(6797):747–52.
5. Prat A, Pineda E, Adamo B, et al. Clinical implications of the intrinsic molecular subtypes of breast cancer. *Breast*. 2015;24:S26–35.
6. Derakhshan F, Reis-Filho JS. Pathogenesis of Triple-negative breast Cancer. *Annu Rev Pathol*. 2022;17:181–204.
7. Yu Y, Yan Y, Niu F, et al. Ferroptosis: a cell death connecting oxidative stress, inflammation and cardiovascular diseases. *Cell Death Discovery*. 2021;7(1):193.
8. Zhou Q, Meng Y, Li D, et al. Ferroptosis in cancer: from molecular mechanisms to therapeutic strategies. *Signal Transduct Target Therapy*. 2024;9(1):55.
9. Passarella D, Ciampi S, Di Liberto V et al. Low-density lipoprotein receptor-related protein 8 at the crossroad between Cancer and Neurodegeneration. *Int J Mol Sci*. 2022;23(16).
10. Li Z, Ferguson L, Deol KK, et al. Ribosome stalling during selenoprotein translation exposes a ferroptosis vulnerability. *Nat Chem Biol*. 2022;18(7):751–61.
11. Lin CC, Lo MC, Moody R, et al. Targeting LRP8 inhibits breast cancer stem cells in triple-negative breast cancer. *Cancer Lett*. 2018;438:165–73.
12. Maire V, Mahmood F, Rigault G, et al. LRP8 is overexpressed in estrogen-negative breast cancers and a potential target for these tumors. *Cancer Med*. 2019;8(1):325–36.

Publisher's note

Springer Nature remains neutral with regard to jurisdictional claims in published maps and institutional affiliations.